The LINNEAN SOCIETY of London BIOLOGICAL Journal of the Linnean Society

Biological Journal of the Linnean Society, 2012, **106**, 607–622. With 7 figures

The homology and origins of intermuscular bones in fishes: phylogenetic or biomechanical determinants?

NICOLE DANOS[1]* and ANDREA B. WARD[2]

[1]*Museum of Comparative Zoology, Harvard University, Cambridge, MA 02138, USA*
[2]*Biology Department, Adelphi University, Garden City, NY 11530, USA*

Received 27 October 2011; revised 18 January 2012; accepted for publication 18 January 2012

Fish body muscles are arranged along the vertebral column in three-dimensional W-shaped blocks, called myomeres. Each myomere is separated from its neighbours by a collagenous sheet, the myoseptum, and embedded in these myosepta and in positions that are conserved throughout gnathostome evolution are distinct tendons. Within teleosts these tendons often ossify. Ossification is usually intramembranous but cartilaginous structures within the tendons have also been reported. Ossified myoseptal tendons are homologous to intermuscular bones and appear only in teleosts. The phylogenetic signal of myoseptal tendon ossfication has not been tested previously, although the presence and morphology of intermuscular bones have been used to infer phylogenetic relationships. We sample over a broad phylogenetic range of teleost fishes to test for (1) the effects of phylogenetic history on the presence of intermuscular bones and (2) morphological correlations with the presence of intermuscular bones. Body shape and fin position as well as vertebral number and aspect ratio are characters that are likely to affect the distribution of stresses along myoseptal tendons, and are therefore good functional predictors of myoseptal tendon ossification. We use the summary information by Patterson & Johnson for a list of species with intermuscular bones and reanalyse the homology of intermuscular bones to myoseptal tendons. We find that there is a phylogenetic signal in the distribution of four out of six ossified tendons, but that after correcting for phylogenetic relationships there are still morphological predictors for the presence of all ossified tendons. *Biological Journal of the Linnean Society*, 2012, **106**, 607–622.

ADDITIONAL KEYWORDS: intramembranous ossification – myosepta – ossified tendons – swimming.

INTRODUCTION

It is astonishing to find that fishes perform nearly every imaginable way of locomotion despite their basal gnathostome body plan. There are fishes that swim in open water and fishes that swim in highly structured habitats; fishes that walk on the bottom of the ocean and fishes that fly above it. To perform each of these unique modes of locomotion, fishes have also attained a variety of body shapes. Yet after more than 100 years of research on fish locomotion, there is still plenty to learn about the basic functions of all the components in the locomotor system of fishes. This system comprises muscle blocks, the myomeres, arranged along the vertebral column and separated by collagenous sheaths, the myosepta. The right side of the body is separated from the left side by the vertical septum, which connects to the vertebral neural spines in the epaxial region and the hemal spines in the hypaxial region. A horizontal septum separates the epaxial from the hypaxial halves of the myomeres. Along the horizontal septum under the skin oriented longitudinally are bundles of red muscle (Gemballa, 2001). The arrangement of these muscle–connective tissue units is further complicated by the angles at which the muscle fibres intersect with each septum (Gemballa & Vogel, 2002).

All gnathostomes have three sets of myoseptal tendons and two sets of tendons that are found within the horizontal septum (Gemballa *et al.*, 2003). Although these structures do not always connect muscle fibres directly to bone they are still referred

*Corresponding author. Current address: Ecology and Evolutionary Biology, University of California Irvine, CA 92697-2525, USA. E-mail: ndanos@uci.edu

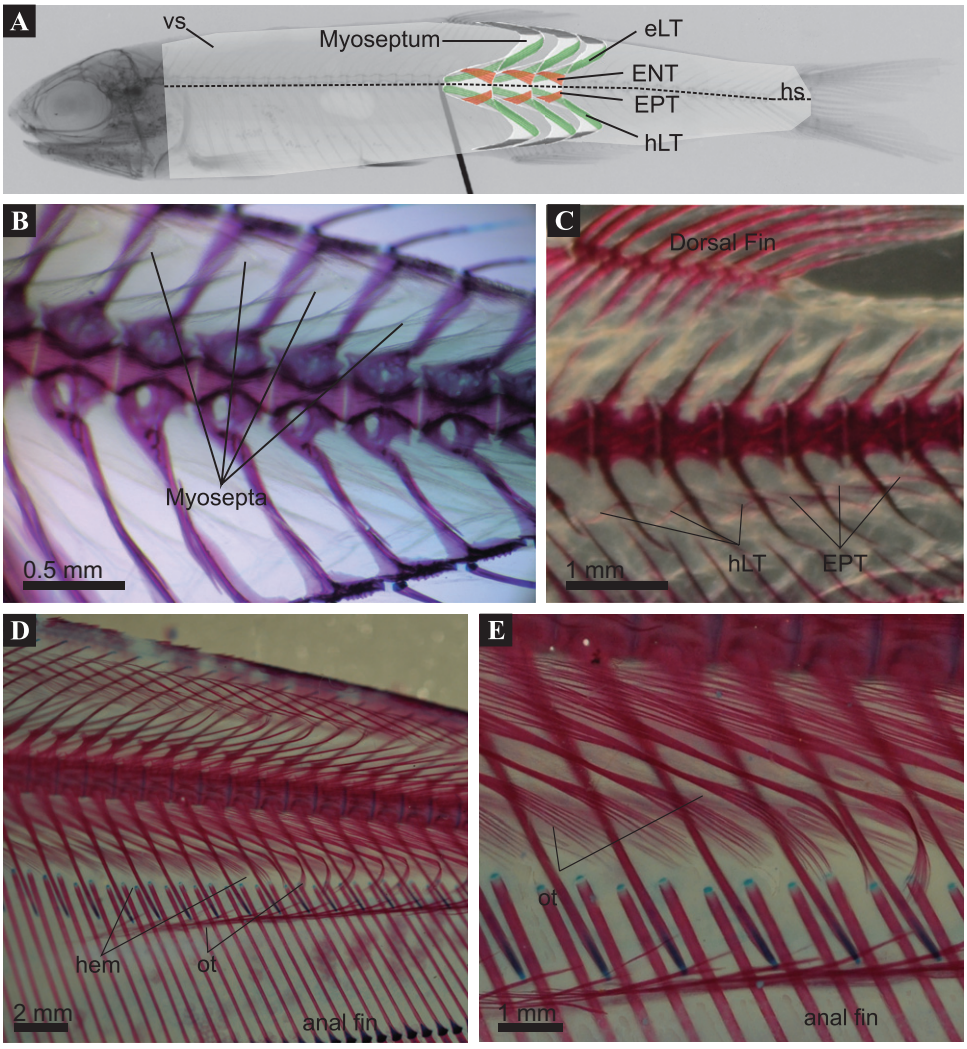

Figure 1. Myoseptal tendon architecture and examples of ossified myoseptal tendons. A, schematic of the horizontal septum (hs, dotted line), vertical septum (vs, light grey sheet) and three post-abdominal myosepta superimposed on an X-ray image of an anchovy, *Anchoa delicatissima*. Tendons are coloured into the myosepta; epineural (ENT) and epipleural tendons (EPT) are orange, lateral tendons are green, myorhaboid tendons are grey. B, lateral view of the myosepta in a cleared and stained juvenile zebrafish, *Danio rerio*. The tendons in this region are either not ossified yet, or are poorly ossified and hence not visible with this staining and imaging technique. C, ossified tendons in the hypaxial midbody region of an adult *D. rerio*. Note that the ossification of the hypaxial lateral tendon (hLT) and the epipleural tendon (EPT) give the resulting intermuscular bone a Y-shaped appearance. Lateral view, cleared and stained specimen. D, midbody region of a clown knifefish, *Apteronotus albifrons*. Hem, hemal spine; ot, ossified tendon. E, close-up of ossified tendon (ot) showing their brush-like morphology.

to as tendons as they are areas distinctly thicker within the collagenous myosepta (Gemballa *et al*., 2003; Gemballa & Roeder, 2004; Danos, Fisch & Gemballa, 2008). Furthermore, in teleosts, some or all of these tendons can ossify along parts of the body (Fig. 1; Gemballa *et al*., 2003). In the case of the epineural or epipleural tendons (Fig. 1A) the collagenous unossified region of the tendon then connects a bone (the ossified tendon) to the vertebra and according to some researchers should therefore be termed ligaments (e.g. Westneat *et al*., 1993; Patterson & Johnson, 1995). However, to facilitate comparative discussions we prefer to maintain the term tendon for the conserved regions of the septa that are significantly thicker than the surrounding tissue (e.g. Gemballa *et al*., 2003; Danos *et al*., 2008). Ossified myoseptal tendons have also been called epineural or accessory ribs and are collectively referred to as intermuscular bones (e.g. Gemballa & Britz, 1998).

Although there have been numerous discussions regarding the functions of myoseptal tendons, there is limited experimental evidence. The functional morphology of the horizontal septum tendons in scombroid fishes, however, has been examined in detail (Westneat *et al*., 1993). These fish typify the carangiform and thunniform swimming modes, with stiff bodies that show little lateral undulation during steady swimming. They also show extreme adaptations of internal anatomy with internalized red muscle, elongated anterior-pointing cones of myosepta and hence elongated lateral tendons which form the medial caudal tendon and the great lateral tendon in tunas (Westneat *et al*., 1993). There is good reason to suspect that the horizontal septum acts in force transmission at least during steady swimming, as it connects the red muscle to the backbone. Indeed, a simple modelling approach by Westneat *et al*. (1993) shows that this function is possible. The authors also suggest that the myosepta as well as the skin are kept under tension due to the contracting muscles and hence may be transferring that tension towards the tail. Donley *et al*. (2004) found that lamnid sharks and tunas, both thuniform swimmers, had similarly elongated and internalized lateral tendons.

Theoretical work has focused on three myoseptal tendon functions: (1) the transmission of force between muscle segments (Long *et al*., 2002), (2) increasing overall body stiffness (Long & Nipper, 1996), and (3) constraining myomere deformation during contraction (Azizi, Gillis & Brainerd, 2002; Brainerd & Azizi, 2005). Interestingly, there has also been a suggested non-locomotor function for ossified myoseptal tendons: storing and releasing energy during sound production in the fawn cusk-eel, *Lepophidium profundorum* (Fine *et al*., 2007).

Although variation in the number of ossified tendons has been demonstrated to be partly under genetic control (e.g. bothid fishes and the common carp; Chanet, Chapleau & Desoutter, 2004; Vallod & Arthaud, 2009), there has not been an independent test to assess the effect of phylogeny on the distribution of ossified myoseptal tendons within actinopterygian fishes. Instead similarities in intermuscular bone morphology have been used to determine phylogenetic relationships. A test of phylogenetic independence is therefore crucial if we are to examine the potential function of myoseptal tendons, ossified or not, using the rich morphological data available.

Here we reanalyse the most comprehensive piece of work on the subject (Patterson & Johnson, 1995) with the aim of asking whether there are any biomechanical predictors of tendon ossification after phylogeny is taken into account. We hypothesize that morphological variables, which describe body shape and fin placement, affect the distribution of forces experienced by the fish body during locomotion and would therefore explain the variation in ossification observed within teleosts. We made specific predictions about the morphological variables that may affect the required material properties of myoseptal tendons by considering the placement of these tendons within the myoseptal architecture. The epineural (ENT) and epipleural (EPT) tendons extend mediolaterally and at an angle to the horizontal septum (Gemballa *et al*., 2003), in a position that can resist torsion of the body. Evidence of rotation along the vertebral column and hence torsion on the surrounding tissue has been collected using X-ray reconstruction of moving morphology (XROMM) technology (Brainerd *et al*., 2010; Nowroozi & Brainerd, 2010). We predict that the position of the median fins, the action of which may put the body under such torsion (e.g. Standen & Lauder, 2007), would necessitate a stiffer epineural or epipleural tendon and may thus be a factor in the ossification of these tendons. The lateral tendon (eLT and hLT for the epaxial and hypaxial region, respectively), on the other hand, is positioned nearly parallel to the vertebral column and spans the distance between the anteriorly pointing and posteriorly pointing cones of the myosepta (Gemballa *et al*., 2003). It has already been demonstrated that the morphology of this tendon correlates with swimming mode (Gemballa & Treiber, 2003; Donley *et al*., 2004; Shadwick & Gemballa, 2006) and is convergent in tunas and lamnid sharks (Donley *et al*., 2004). Therefore, morphological metrics such as body aspect ratio and vertebral number that influence the stiffness of the whole body (Long & Nipper, 1996) should also correlate with the presence or absence of tendon ossification. The same variables should also affect the required material properties of the horizontal septum tendons as they are oriented anteroposteriorly. The third pair of myoseptal tendons, the myorhabdoid, ossify only rarely (e.g. in *Anchoa compressa* and the genus *Sternorhynchus*; Chapman, 1944; De Santana & Vari, 2010) and data on their ossification is not included in Patterson & Johnson (1995) because the ossifications were assumed to be autapomorphic characters for the taxa in which they occur. Although further analysis of the myorhabdoid tendons is not included here, given the tendon's position at the distal ends of the myosepta and the acute angles at which it intersects with muscle fibres (Gemballa & Vogel, 2002) we predict that increased stiffness will only be required in cases where that region of the myoseptum is greatly elongated. In this way the increased moment arm of this tendon can compensate for the reduced longitudinal force transmission by the acute angles of insertion of the muscle fibres.

MATERIAL AND METHODS

MORPHOLOGICAL DATA: INTERMUSCULAR BONES

Data on the presence and distribution along the body of intermuscular bones were obtained from Patterson & Johnson (1995). To determine homology between the intermuscular bones of Patterson & Johnson (1995) and myoseptal tendons we used the myoseptal architecture as summarized in Gemballa *et al*. (2003). In the epaxial and hypaxial myoseptal regions, intermuscular bones that inserted into the vertebrae or pointed mediolaterally were interpreted as ossified epineural tendons (Fig. 1). Forked epineural or epipleural bones in Patterson & Johnson were interpreted as an ossification along both the epineural (epaxially) or epipleural (hypaxially) and the lateral tendons. In cases of forked epineurals or epipleurals where the medial attachment to the vertebral column is lost and the intermuscular bone runs parallel to the vertebral column, the bone was interpreted as an ossified lateral tendon.

Any intermuscular bone in the horizontal septum was recorded as an epicentral bone. This strict interpretation also avoided the introduction of phylogenetic bias to the dataset, as Patterson & Johnson (1995) identify certain epineural and epipleural bones as having moved to the horizontal septum based on comparisons with closely related species.

For each species provided within the summary work of Patterson & Johnson (1995) and also found at the Museum of Comparative Zoology (Harvard University) we noted from Patterson & Johnson (1) the condition of each myoseptal tendon: ossified, not ossified or cartilaginous, (2) the vertebral segments that accompany ossified or cartilaginous tendons, (3) the portion of the vertebral column that bears ribs, and (4) the standard length and number of vertebrae of each specimen used by the authors for their description. The species included in our study are listed in Table 1.

MORPHOLOGICAL DATA: BODY SHAPE AND FIN POSITIONS

Body shape data were collected from photographs and X-ray images of specimens from the Museum of Comparative Zoology, Harvard University (Table 1). Photographs were taken using a Nikon D70 and a 55-mm lens. From these images we recorded the specimen's standard length (SL), snout–vent length (SVL), distance from the tip of the upper jaw to the insertion of each fin (e.g. pre-pectoral is the distance from the tip of the maxilla to the insertion of the pectoral fin), height of the pectoral fin from the ventral margin of the body, maximum body height, distance from the tip of the upper jaw to the position of maximum body height (Fig. 2), and maximum body width. All measurements were normalized to SL.

Each specimen was also X-rayed at the Museum of Comparative Zoology Digital Imaging Facility at Harvard University using an INSPEX 20i digital X-ray system with Kevex PXS10-16W micro-focus X-ray source and Varian PaxScan 4030R panel and software (compiled by Kodex, Inc.). From each X-ray image we quantified the following: (1) number of vertebrae, (2) number of rib-bearing vertebrae, (3) distance from the tip of the maxilla to the end of the last rib-bearing vertebra, (4) vertebral length of the first caudal vertebra (length from the anterior to the posterior margins of the vertebra), and (5) vertebral height of the first caudal vertebra (mean height along the anterior and posterior vertebral margins). Vertebral aspect ratio was then calculated as the vertebral length divided by vertebral height.

PHYLOGENETIC ANALYSIS: ANCESTRAL CHARACTER RECONSTRUCTION AND COMPARATIVE METHODS

A tree topology was inferred from published trees of smaller groups (Fig. 3; Johnson & Patterson, 1993; Moore, 1993; Baldwin & Johnson, 1996; Hilton, 2003; Santini & Tyler, 2003; Nelson, 2006; Kawahara *et al*., 2008; Santini *et al*., 2009; Yagashita *et al*., 2009; Lavoue, Miya & Nishida, 2010). Branch lengths were

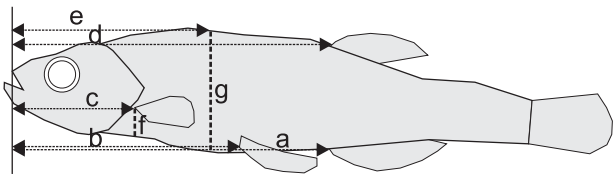

Figure 2. Body morphology measurements taken from photographs of museum specimens. For each specimen we measured the distance from the tip of the upper jaw to insertion of the anal (a), pelvic (b), pectoral (c), and dorsal (d) fins. We also measured the maximum height of the body (g) and the distance from the tip of the upper jaw to the point of maximum height (e). Additionally, we measured the height of the pectoral fin (f) and standard and snout–vent length. From a dorsal image of the specimen we also measured maximum body width.

Figure 3. Distribution of tendon ossification on a supertree compiled from published family-level phylogenies ($n = 88$ taxa). Taxa with ossified tendons are accompanied by coloured square symbols. ENT, epineural; EPT, epipleural; POT, posteriorly oriented tendon; AOT, anteriorly oriented tendon; eLT, epaxial lateral tendon; hLT, hypaxial lateral tendon.

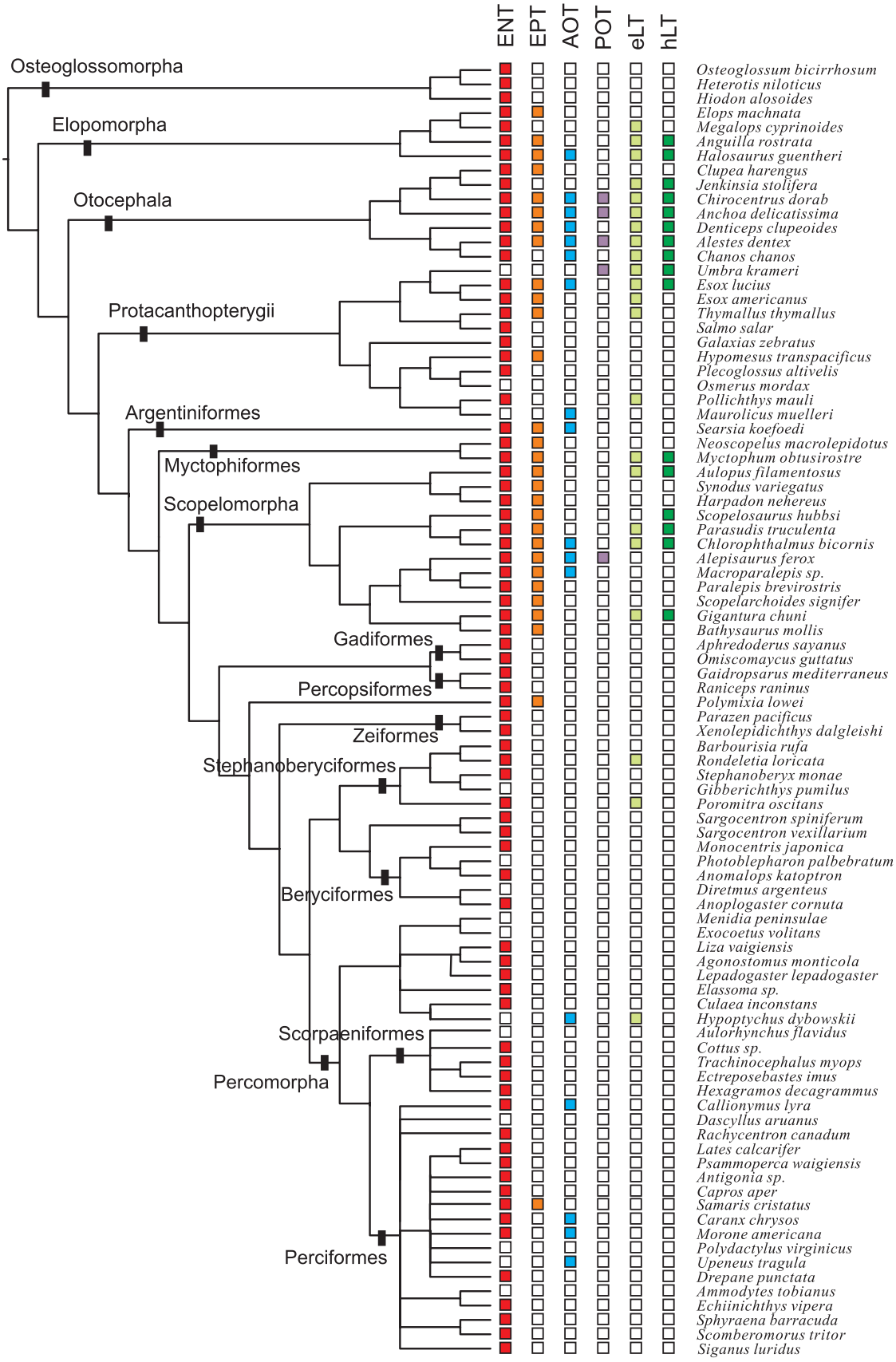

Table 1. Proportion of body with myoseptal tendon ossification

Family	Genus	Species	MCZ no.	SL (mm)	ENT	Body prop.	eLT	Body prop.	POT	Body prop.	AOT	Body prop.	EPT	Body prop.	hLT	Body prop.
Osteoglossomorpha																
Arapaimidae	*Heterotis*	*niloticus*	4006	203	1	0.02–0.53	0		0		0		1	0.42–0.52	0	
Hiodontidae	*Hiodon*	*alosoides*	17697	212	1	0.02–0.51	0		0		0		0		0	
Osteoglossidae	*Osteoglossum*	*bicirrhosum*	99472	266	1	0.01–0.39	0		0		0		0		0	
Elopomorpha																
Anguillidae	*Anguilla*	*rostrata*	2534	156	1	0.009–0.77	0		0		0		1	0.33–0.78	0	
Halosauridae	*Halosaurus*	*guentheri*	164501	414	1	0.01–0.32	1	0.06–0.75	0		0		0		1	0.30–0.73
Elopidae	*Elops*	*machnata*	30801	234	1	0.50–0.72	1	0.03–0.95	0		0		1	0.48–0.70	1	0.52–0.95
Megalopidae	*Megalops*	*cyprinoides*	18112	163	1	0.01–0.67	1	0.45–0.94	1	0.01–0.67	0		1	0.01–0.63	1	0.46–0.90
Otocephala																
Alestiidae	*Alestes*	*dentex*	4016	102	0		1	0.02–0.93	0		0		0		1	0.33–0.93
Engraulidae	*Anchoa*	*delicatissima*	17993	61	1	0.03–0.80	1	0.83–1.00	1	0.08–0.55	2	0.05–0.33	1	0.13–0.83	1	0.10–1.00
Chanidae	*Chanos*	*chanos*	56538	167	1	0.05–0.67	1	0.05–0.95	1	0.02–0.58	1	0.02–0.37	1	0.47–0.70	1	0.37–0.56
Chirocentridae	*Chirocentrus*	*dorab*	5934	282	1	0.07–0.69	1	0.07–0.99	1	0.04–0.85	0		1	0.21–0.75	1	0.01–0.99
Clupeidae	*Clupea*	*harengus*	17646	187	1	0.02–0.78	1	0.45–0.95	1	0.02–0.59	1	0.02–0.40	1	0.03–0.78	1	0.48–0.91
Denticipitidae	*Denticeps*	*clupeoidus*	56428	36	1	0.51–0.67	1	0.56–0.97	1	0.05–0.54	0		1	0.49–0.72	1	0.51–0.97
Clupeidae	*Jenkinsia*	*stolifera*	17944	51	1	0.08–0.84	1	0.55–1.00	1	0.03–0.61	1	0.03–0.58	1	0.58–0.87	1	0.05–0.95
Protacanthopterygii																
Esocidae	*Esox*	*americanus*	168471	171	1	0.13–0.78	1	0.02–0.67	0		0		1	0.43–0.78	0	
Esocidae	*Esox*	*lucius*	26319	292	1	0.02–0.75	1	0.11–0.67	0		0		1	0.57–0.67	0	
Galaxiidae	*Galaxias*	*zebratus*	58707	46	1	0.02–0.70	0		0		0		1	0.48–0.70	0	
Osmeridae	*Hypomesus*	*transpacificus*	147932	138	1	0.02–0.56	0		0		0		0		0	
Sternoptychidae	*Maurolicus*	*muelleri*	58809	55	1	0.3	0		1	0.03–0.27	0		1	0.36–0.61	0	
Osmeridae	*Osmerus*	*mordax*	39848	214	1	0.02–0.59	1	0.30–0.33	0		0		0		0	
Osmeridae	*Plecoglossus*	*altivelis*	29028	114	0		0		0		0		0		0	
Phosichthyidae	*Pollichthys*	*mauli*	56954	47	0		0		1	0.02–0.38	0		0		0	
Salmonidae	*Salmo*	*salar*	57694	286	1	0.02–0.55	0		0		0		0		0	
Platytroctidae	*Searsia*	*koefoedi*	100979	142	1	0.53–0.60	0		1	0.02–0.51	0		1	0.07–0.53	0	
Salmonidae	*Thymallus*	*thymallus*	6947	257	1	0.04–0.41	0		0	0.04–0.14	0		0		0	
Umbridae	*Umbra*	*krameri*	46455	82	1	0.03–0.83	1	0.63	0		0		1	0.57–0.86	1	0.63
Myctophiformes																
Myctophidae	*Myctophum*	*obtusirostre*	105814	74	1	0.03–0.81	1	0.47–0.92	0		0		1	0.36–0.81	1	0.56–0.92
Neoscopelidae	*Neoscopelus*	*macrolepidotus*	28159	152	1	0.03–0.74	1	0.48–0.87	0		0		1	0.42–0.71	1	0.52–0.87
Scopelomorpha																
Alepisauridae	*Alepisaurus*	*ferox*	164377	552	1	0.12–0.61	0		1	0.12–0.59	1	0.02–0.12	1	0.02–0.53	0	
Aulopidae	*Aulopus*	*filamentosus*	40821	350	1	0.02–0.70	0		0		0		1	0.06–0.72	0	
Bathysauridae	*Bathysaurus*	*mollis*	40518	212	1	0.69–0.73	0		0		0		1	0.02–0.73	0	
Chlorophthalmidae	*Chlorophthalmus*	*bicornis*	57381	110	1	0.02–0.80	1	0.34–0.95	0		0		1	0.05–0.75	1	0.95
Giganturidae	*Gigantura*	*chuni*	185926	116	1	0.03–0.93	1	0.03–0.93	0		0		1	0.03–0.83	1	0.03–0.43
Synodontidae	*Harpadon*	*nehereus*	45317	187	1	0.24–0.79	0		0		0		1	0.05–0.76	0	
Paralepididae	*Macroparalepis*	*sp.*	164799	117	1	0.02	0		0		0		1	0.01–0.05	0	
Paralepididae	*Paralepis*	*brevirostris*	164788	62	1	0.03–0.56	0		0		0		1	0.05–0.50	0	
Chlorophthalmidae	*Parasudis*	*truculenta*	166072	141	1	0.03–0.79	1	0.28–0.79	1	0.03–0.70	0		1	0.05–0.77	1	0.44–0.77
Scopelarchidae	*Scopelarchoides*	*signifer*	127124	102	1	0.02–0.56	0		0		0		1	0.02–0.52	0	
Notosudidae	*Scopelosaurus*	*hubbsi*	158749	323	1	0.02–0.62	0		0		0		1	0.03–0.59	1	0.34–0.41
Synodontidae	*Synodus*	*variegatus*	36737	117	1	0.01–0.64	0		0		0		1	0.03–0.61	0	
Percopsiformes + Gadiformes																
Aphrredoderidae	*Aphredoderus*	*sayanus*	59950	97	1	0.03–0.28	0		0		0		0		0	
Phycidae	*Gaidropsarus*	*mediterraneus*	64300	123	1	0.07–0.58	0		0		0		0		0	
Percopsidae	*Omiscomaycus*	*guttatus*	6866	79	1	0.03–0.17	0		0		0		0		0	
Gadidae	*Raniceps*	*raninus*	12378	308	1	0.04–0.24	0		0		0		0		0	

Polymixiiformes															
Polymixiidae	*Polymixia*	*lowei*	76010	167	1	0.03–0.69	0		0		0		1	0.10–0.41	0
Zeiformes															
Parazenidae	*Parazen*	*pacificus*	40612	91	1	0.04–0.52	0		0		0		0		0
Grammicolepididae	*Xenolepidichthys*	*dalgleishi*	51303	74	1	0.05–0.19	0		0		0		0		0
Stephanoberyciformes															
Barbourisiidae	*Barbourisia*	*rufa*	41340	150	1	0.02–0.12	0		0		0		0		0
Gibberichthyidae	*Gibberichthys*	*pumilus*	54368	78	1	0.03–0.28	0		0		0		0		0
Melamphaidae	*Poromitra*	*oscitans*	97463	74	1	0.04–0.16	0		0		0		0		0
Rondeletiidae	*Rondeletia*	*loricata*	165903	110	1	0.05–0.53	2	0.05–0.42	0		0		0		0
Stephanoberycidae	*Stephanoberyx*	*monae*	52935	87	0		0		0		0		0		0
Beryciformes															
Anomalopidae	*Anomalops*	*katoptron*	56858	76	0		0		0		0		0		0
Anoplogasteridae	*Anoplogaster*	*cornuta*	151384	139	0		0		0		0		0		0
Diretmidae	*Diretmus*	*argenteus*	49115	41	1	0.03	0		0		0		0		0
Anomalopidae	*Photoblepharon*	*palbebratum*			0		0		0		0		0		0
Holocentridae	*Sargocentron*	*spinifer*	43587	97	1	0.04–0.56	2	0.04–0.15	0		0		0		0
Holocentridae	*Sargocentron*	*vexillarium*			1		0		0		0		0		0
Monocentridae	*Monocentris*	*japonica*	27251	113	1	0.31–0.42	0		0		0		0		0
Percomorpha															
Mugilidae	*Agonostomus*	*monticola*	33126	135	1	0.04–0.21	0		0		0		0		0
Ammodytidae	*Ammodytes*	*tobianus*	12462	116	0		0		1	0.02–0.63	0		0		0
Caproidae	*Antigonia*	sp.			1		0		0		0		0		0
Aulorhynchidae	*Aulorhynchus*	*flavidus*	145481	141	0		0		0		0		0		0
Callionymidae	*Callionymus*	*lyra*	64317	83	1	0.10–0.40	0		0		0		0		0
Caproidae	*Capros*	*aper*	52884	45	1	0.09–0.57	0		0		0		0		0
Carangidae	*Caranx*	*chrysos*	26305	203	1	0.04–0.64	0		0		0		0		0
Cottidae	*Cottus*	sp.	78122	59	1	0.03–0.45	0		0		0		0		0
Gasterosteidae	*Culaea*	*inconstans*	49602	43	1	0.03–0.48	0		0		0		0		0
Pomacentridae	*Dascyllus*	*aruanus*	51671	83	0		0		1	0.04–0.62	0		0		0
Drepaneidae	*Drepane*	*punctata*	46556	59	1	0.04–0.46	0		0		0		0		0
Trachinidae	*Echiichthys*	*vipera*			1		0		0		0		0		0
Scorpaenidae	*Ectreposebastes*	*imus*	164078	79	1	0.04–0.33	0		0		0		0		0
Elassomatidae	*Elassoma*	sp.	91458	23	1	0.04–0.46	0		0		0		0		0
Exocoetidae	*Exocoetus*	*volitans*	737	130	1	0.02–0.64	0		0		0		0		0
Hexagrammidae	*Hexagrammos*	*decagrammus*	13991	157	1	0.02–0.48	0		0		0		0		0
Hypoptychidae	*Hypoptychus*	*dybowskii*	32494	66	0		0		0		0		0		0
Latidae	*Lates*	*calcarifer*	25774	496	1	0.04–0.16	0		0		0		0		0
Gobiesocidae	*Lepadogaster*	*lepadogaster*	137450	60	1	0.06–0.58	0		0		0		0		0
Mugilidae	*Liza*	*vaigiensis*	30515	145	1	0.04–0.13	0		0		0		0		0
Atherinopsidae	*Menidia*	*peninsulae*	36338	39	0		0		0		0		0		0
Moronidae	*Morone*	*americana*	2893	105	1	0.04–0.28	0		0		0		0		0
Polynemidae	*Polydactylus*	*virginicus*	92071	134	0		0		1	0.04–0.29	0		0		0
Latidae	*Psammoperca*	*waigiensis*	36902	155	1	0.04–0.32	0		0		0		0		0
Rachycentridae	*Rachycentron*	*canadum*	33119	78	1	0.04–0.52	0		0		0		0		0
Samaridae	*Samaris*	*cristatus*	32979	111	1	0.05–0.95	1	0.10–0.79	1	0.03–0.23	0		1	0.13–0.77	0
Scombridae	*Scomberomorus*	*tritor*	17178	167	1	0.02–0.45	0		0		0		0		0
Siganidae	*Siganus*	*luridus*	30815	151	1	0.04–0.43	0		0		0		0		0
Sphyraenidae	*Sphyraena*	*barracuda*	uncatalogued	252	1	0.04–0.12	0		0		0		0		0
Scorpaenidae	*Trachinocephalus*	*myops*	48741	137	1	0.02–0.80	0		0		0		1	0.04–0.81	0
Trachinidae	*Echiichthys*	*vipera*	12902	106	1	0.03–0.54	0		0		0		0		0
Mullidae	*Upeneus*	*tragula*	59278	179	0		0		1	0.04–0.54	0		0		0
Total number of species with ossification:					74		20 (+2 cartilage)		18		3 (+1 cartilage)		33		17

Tendon ossification data reinterpreted from Patterson & Johnson (1995). Body morphometrics collected from the listed museum specimens. MCZ no., Museum of Comparative Zoology catalogue number; SL, standard length; body proportion, relative start and end location of tendon ossification; 0, no ossification; 1, ossified tendon; 2, cartilaginous tendon.

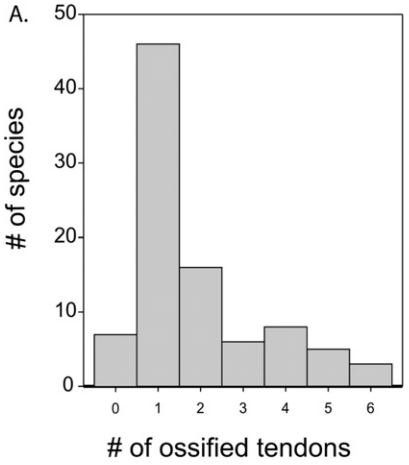

B.

	Epaxial	Hypaxial	Horizontal
Epaxial	42	24	1
Hypaxial		0	0
Horizontal			5
All regions		11	

Figure 4. Number of ossified tendons. A, count of species in our sample versus number of ossified tendons. B, number of species with ossified tendons by myoseptal region (epaxial, hypaxial, or in the horizontal septum). Seven species in this sample have zero ossified tendons.

estimated in the open source computer language R, using *compute.brlen* (written by Julien Dutheis & Emannuel Paradis).

Ancestral character states of tendons (ossified, tendinous, or cartilaginous) were reconstructed for all nodes in R using the *ace* function (written by Emmanuel Paradis & Ben Bolker).

The strength of phylogenetic signal was assessed in the open source program R using Pagel's lambda as a signal metric (Pagel, 1999). The *fitDiscrete* function (written by Luke J. Harmon & Richard E. Glor) was used to estimate lambda for the presence or absence of ossification at each tendon locus, while the *fitContinuous* function (written by Luke J. Harmon & Wendell Challenger) was used to assess the phylogenetic signal in the first four principal components that describe body shape and fin placement (obtained in JMP, Version 8, SAS Institute Inc.). A lambda value of 0 suggests no phylogenetic signal while a lambda value of 1 suggests an entirely phylogenetically dependent character distribution. Because the lambda estimating functions require no zero-length branches in the phylogeny any unresolved terminal polytomies in the recovered teleost phylogeny were randomly resolved (function *multi2di*, written by Emmanuel Paradis) before the fitting functions were applied.

Analysis of variance and principal components analysis (PCA)

PCA was carried out on the raw 11 body shape variables measured from the photographic and X-ray images using JMP 8 (SAS Institute Inc.). It was also carried out on the phylogenetically corrected values obtained using the *pic* function in R (written by Emmanuel Paradis). Both approaches were used in order to facilitate future comparisons with the taxa in this study even if phylogenetic information is not available. The correlations between phylogenetically corrected variables were also obtained from the PCA.

To correlate raw morphological variables and the presence or absence of ossification at each tendon locus a phylogenetic ANOVA was carried out in R for each tendon and each morphological variable (function *phy.manova* written by Luke Harmon).

RESULTS

Comparative morphology of intermuscular bones

In the sample of the 88 species included in this study, the greatest number of species have only one of the six tendons ossified, seven species have no ossified tendons, and three species have all six tendons ossified (Figs 3, 4). In the vast majority of cases where only one tendon is ossified (42/47) that tendon is in the epaxial region and there are no instances when the only ossified tendon is a hypaxial one (Figs 3, 4). Also, taxa with ossification in the hypaxial and horizontal septum tendon always have an ossification in the epaxial tendon (Fig. 3).

The epineural tendon when ossified was present along 0.07 ± 0.12 to 0.49 ± 0.25 of the vertebral column length (mean ± SEM), while the ossified epipleural tendon started at 0.22 ± 0.20 and ended at 0.65 ± 0.16 of vertebral length (Fig. 5). The ossified anteriorly oriented tendon (AOT) runs between 0.05 ± 0.04 and 0.37 ± 0.16 while the posteriorly oriented tendon (POT) runs between 0.03 ± 0.02 and 0.48 ± 0.22 (Fig. 5). The lateral tendon in the epaxial region was ossified between 0.26 ± 0.25 and

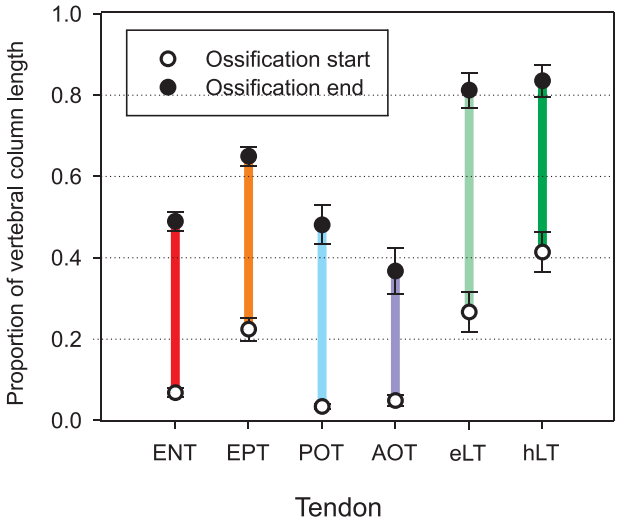

Figure 5. Body regions with ossified tendons. Mean and SEM start and end point of all taxa. On the *y*-axis, zero is the anterior margin of the first vertebra; 1.0 is the last caudal vertebra.

0.81 ± 0.21 and between 0.41 ± 0.23 and 0.84 ± 0.18 in the hypaxial region (Fig. 5).

Comparative morphology of body shape

The first four principal components identified by the PCA explained 58% of the variation in body shape. The score plot for the first and second components is presented in Figure 6. The following variables loaded onto component 1 with a loading of more than 0.5: SVL, vertebral count and vertebral aspect ratio. Maximum body height and distance to pectoral fin loaded onto component 1 with a loading smaller than –0.5. No variables loaded negatively onto component 2 with high loading factors but the distance to maximum body height, dorsal, anal, and pelvic fins had loadings higher than 0.5 (Fig. 6).

Three taxa representing body types characteristic of different swimmers are identified in the PCA plot: *Anguilla rostrata*, *Esox lucius*, and *Sphyraena barracuda*. *Anguilla rostrata* had a high positive PC1 but low PC2 score indicative of its relatively high vertebral count (110), and high vertebral aspect ratio (0.67) but low relative body height (0.06). *Esox lucius* and *S. barracuda* fall in different areas of the combined body and fin placement morphospace. Although these are both predatory fish that are good at obtaining high accelerations (deSylva, 1963; Webb, 1978; Porter & Motta, 2004) they differ in the placement of their fins as demonstrated by their PC1 and PC2 scores. The pelvic fins of *S. barracuda* are located more anteriorly than those of *E. lucius* and it has two dorsal fins, the first occurring more anteriorly than the single dorsal fin of *E. lucius*.

The body outlines for the taxa that occupied the most extreme position within each morphospace quadrant are also provided in Figure 6. *Rondeletia loricata*, one of only two species in the family Rondeletiidae (redmouth whalefishes), has a nearly rectangular body with the fins placed far posteriorly on the body. Moving clockwise through the PCA plot, *Osteoglossum bicirrhosum*, the silver arowana, has an overall longer and more elongate body than *Rondeletia* although its lateral profile is similarly rectangular. *Halosaurus guentheri* and *Alepisaurus ferox* are two of the most extremely elongated species in this sample. *Halosaurus* has 250 high-aspect-ratio vertebrae that form a long body tapering into a very thin caudal fin. *Alepisaurus*, on the other hand, has only 53 vertebrae that are longer than they are high and a less elongate body (height/length ratio = 0.11 compared with 0.07 in *Halosaurus*). The *Alepisaurus* body ends in a bifurcating homocercal tail. *Samaris cristatus* is the only flatfish in the examined dataset and has the lowest PC2 score. *Anoplogaster cornuta* falls on the far negative end of the morphospace primarily because of its large body height.

Ossification of the ENT covered the entire morphospace described by the first two principal components (Fig. 6A) but epipleural (EPT) ossification was constrained to the middle values of PC1 (Fig. 6B). Ossification of the lateral tendons (eLT and hLT) was mostly restricted to the middle of PC2 with some extreme exceptions such as *H. guentheri* (Fig. 6C, D). Ossification of the horizontal septum tendons (AOT and POT) did not show much of a pattern on the first two PC axes (Fig. 6E, F).

When the body morphological variables were corrected for phylogeny using the teleost tree generated from the literature (Fig. 3) and then subjected to a PCA, the correlations between individual variables could be assessed. This was important in interpreting the results of the phylogenetic analysis of variance on individual variables.

Phylogenetic signal in myoseptal tendon ossification

The phylogenetic signals of all myoseptal tendon ossifications were assessed using maximum-likelihood estimation of Pagel's lambda. This metric quantified whether the distribution of tendon ossification simply followed the underlying phylogenetic tree pattern or not. Ossification of all tendons except the AOT and hLT had lambda greater than 0.5. When the likelihood score of the model with estimated lambda was compared with the likelihood of a model in which lambda was forced to equal zero, a likelihood ratio was obtained whose distribution can be assumed to approach the distribution of a χ^2 statistic with one

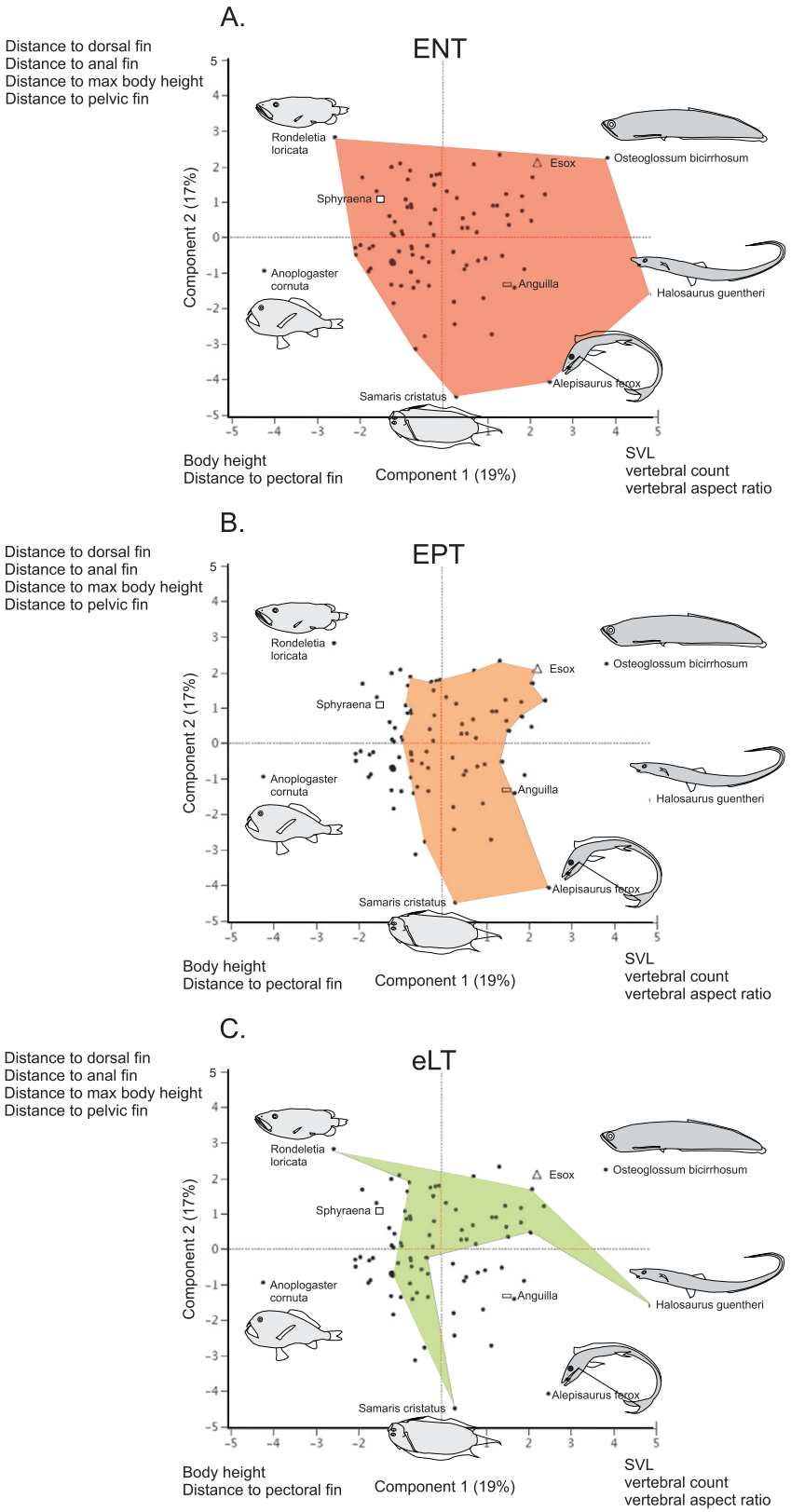

Figure 6. Principal components analysis of body morphometrics. Morphospace occupied by species with tendon ossification is coloured. Extreme data-points are illustrated with body outlines as are well-known body shapes: *Anguilla* (rectangle), *Sphyraena* (square) and *Esox* (triangle). A, ENT; B, EPT; C, eLT; D, hLT; E, AOT; F, POT.

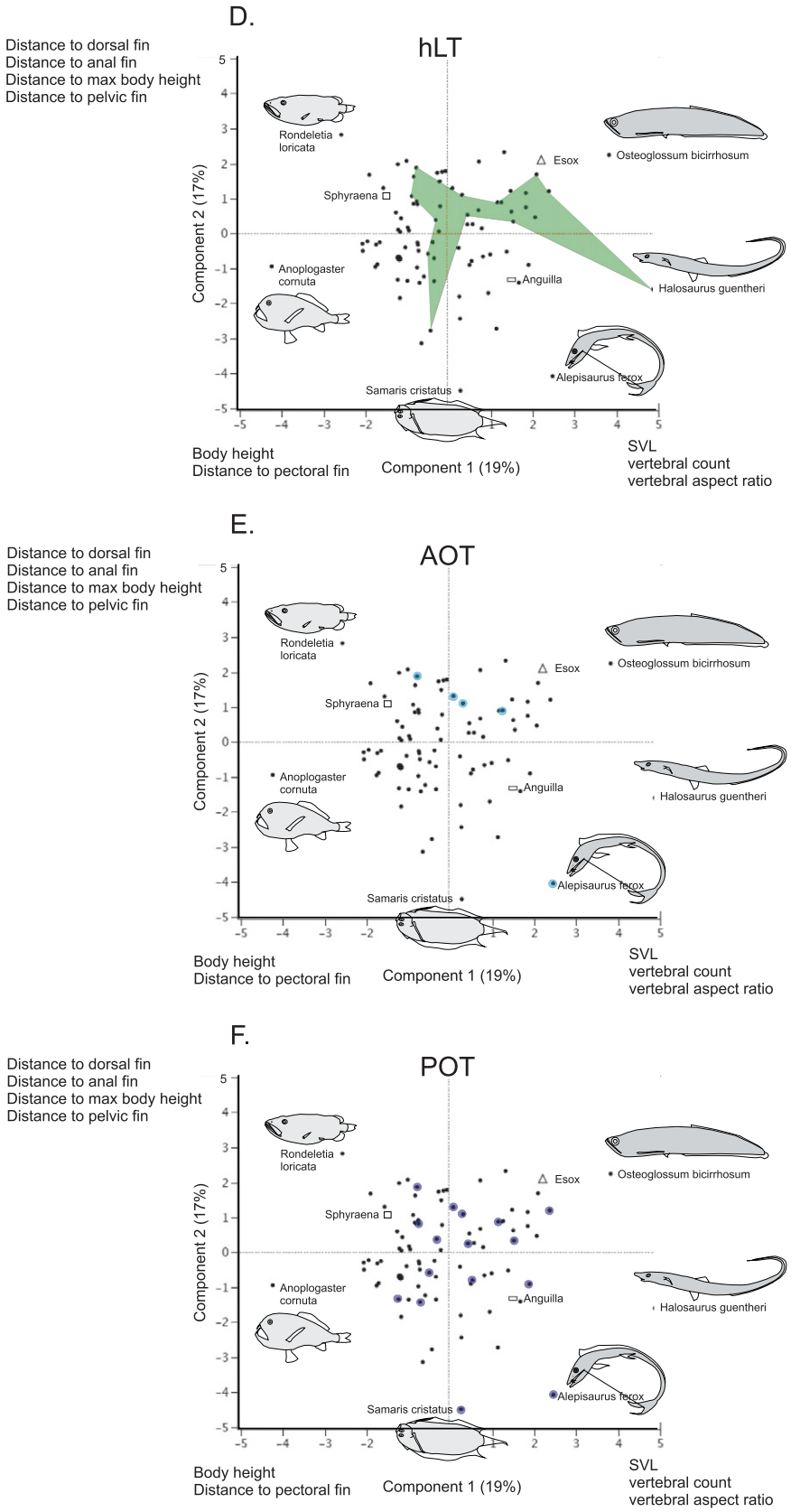

Figure 6. *Continued*

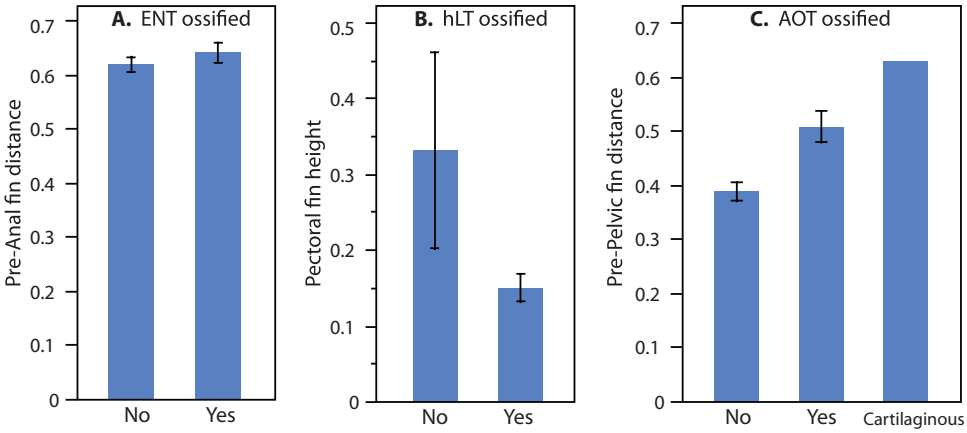

Figure 7. Significant phylogenetic ANOVA results. A, the distance to the insertion of the anal fin (pre-anal distance) was significantly different between species with ossified and unossified epineural tendons, ENT. B, pectoral fin height was significantly lower in species that had an ossified hypaxial lateral tendon, hLT. C, in species with ossified anteriorly oriented tendons, AOT, the distance to the pelvic fin insertion (pre-pelvic distance) was longer than in species with unossified AOT. One species had a cartilaginous AOT and in that case the pre-pelvic distance was even greater.

degree of freedom (Pagel, 1999), allowing us to assign a *P*-value to the lambda estimates. Based on this method, ENT and AOT had no phylogenetic signal ($\lambda = 0$, $P < 0.0001$) while EPT, POT, hLT, and eLT had significant phylogenetic signal ($\lambda = 0.95$, 0.60, 0.94 and 0.91, respectively).

Evolution of myoseptal tendon ossification

The outgroup of all teleosts, *Amia calva*, does not show any myoseptal tendon ossification. The ancestral reconstruction of ossification patterns showed that the likelihood of tendon ossification at the root of the teleost tree was 0.0001 or lower for all tendons except ENT (likelihood < 0.99) and EPT (likelihood = 0.06). All the major clades represented in this study and illustrated in Figure 3 had a likelihood of ENT ossification greater than 0.5. The following clades had a likelihood of EPT ossification that was greater than 0.5: Osteoglossomorpha, Elopomorpha, Myctophiformes, Osmeriformes, and Scopelomorpha. The clades with a likelihood of eLT ossification greater than 0.5 were the Elopomorpha and the Otocephala, while only the Otocephala had a likelihood of POT ossification greater than 0.5. None of the clades identified here had a likelihood of hLT or AOT ossification greater than 0.5 at their base.

Phylogenetic analysis of variance

A phylogenetic ANOVA was conducted to look for differences in the mean values of body shape morphometrics between the groups of taxa that had ossified tendons and those that did not. The ossification of only three tendons showed a significant difference in morphology between species with ossified and unossified tendons. Species with ossified ENT had significantly higher relative preanal fin regions (Fig. 7). Species with ossified hLT had pectoral fins that were positioned lower along the body's dorsoventral axis (Fig. 7), and species with ossified AOT had longer pre-pelvic fin regions (Fig. 7). The species with the only cartilaginous AOT, *Anchoa delicatissima*, had the highest relative pre-pelvic fin region (Fig. 7).

DISCUSSION

The axial locomotor system of fishes is constructed of segmented musculature. Consecutive muscle segments are separated by myosepta and within the myosepta are tendons, known to ossify in a number of species (Patterson & Johnson, 1995). In this study, we examined whether presence of ossified tendons was correlated with body shape measurements or with phylogenetic position. We found that there was phylogenetic signal in ossification as well as significant relationships between body shape parameters and tendon ossification.

Evolution of tendon ossification in teleosts

Patterson & Johnson (1995) suggest that there are short ossified epineurals on the first few vertebrae in the basal actinopterygian palaeoniscoids and in Devonian lungfishes. However, there is no evidence of tendon ossification in extant lungfishes. Additionally, the modern representative of the teleost sister group Amiiformes, *Amia calva* (Lauder & Liem, 1983; Grande & Bemis, 1998), does not show any tendon ossification (Gemballa & Roeder, 2004). Our study

demonstrates that the epineural tendon was indeed present at the root of the teleost tree as suggested by the fossil record, despite the lack of these ossifications in the modern representatives of the teleost sister group. Based on our ancestral state reconstructions, there are a minimum of 11 losses of ENT ossification and multiple origins and possibly losses of ossification for all the other tendons. Although there are multiple evolutionary events associated with tendon ossification, there is nonetheless a strong phylogenetic signal in the distribution of tendon ossifications, as indicated by the values of Pagel's lambda, which were significant for all tendons except the ENT and AOT.

Effect of body shape on tendon ossification

The architecture of myosepta and their tendons was used to make predictions about which body shape and fin placement variables would correlate with tendon ossification. The longitudinal distance of the anal and pelvic fins from the snout correlated with the ossification of the ENT and AOT, even though fin placement was predicted to correlate only with ENT and EPT ossification. However, after also correcting for the phylogenetic signal present in the body shape morphometrics using phylogenetically independent contrasts and then doing a multivariate PCA, it is clear that many of these morphological variables are correlated among themselves. For example, pectoral fin height, which is lower in species with ossified hL, is strongly correlated with maximum body height and hence body aspect ratio (correlation coefficient = 0.82). Some of these correlations are probably based on developmental dynamics (Ward & Brainerd, 2007) such as the proportion of body length occupied by ribbed vertebrae and the total body length, as different groups of actinopterygian fishes have taken different developmental paths to body elongation.

Developmental origins of morphological diversity in intermuscular bones

The gross morphological development of intermuscular bones has been described in only a few cases, and in all cases it was described as undergoing intramembranous ossification (Bird & Mabee, 2003). Yet Patterson & Johnson (1995) found three instances of cartilaginous tendons: the AOT in *Anchoa delicatissima* and the eLT in *Rondeletia loricata* and *Sargocentron spinifer* (Patterson & Johnson, 1995). Primitively, epineurals were thought to have a cartilaginous core and cap (Schaeffer & Patterson, 1984), even though all of the recent teleosts have only solid intramembranous epineurals. Does the change in the process of tendon mineralization from endochondral to intramembranous reflect a developmental shift at the base of the teleost tree or are they due to different types of mechanical loadings that result from the exploration of new body morphospace and new locomotor modes? Or are these skeletal elements not homologous with the intramembranous epicentral bones? Based on the consistent location of these thin, elongate bones in the horizontal septum, parallel to the orientation of the tendons, we conclude that cartilaginous epicentral bones are also homologous to horizontal septum tendons. Why, in these few cases, does ossification go through a cartilaginous phase instead of directly to bone deserves further investigation.

Pleiotropy?

The relative position of fins is a trait strongly controlled by patterning genes (Grandel & Schulte-Merker, 1998; Ruvinsky *et al*., 2000; Mabee *et al*., 2002; Ahn & Ho, 2008). It is therefore possible that the strong correlation between myoseptal tendon ossification and position of fins is the result of pleiotropy. However, further investigation indicates that biomechanics may also be a strong factor behind tendon ossification (Fig. 6). If the body proportion along which a tendon ossifies is due to the expression of homeotic genes, then we would expect an overlap in the regions occupied by the ossified or unossified tendon, and the region before or after a given fin whose position is strongly correlated with ossification. However, there is no such trend for the correlation between dorsal fin position and ossification of the ENT. This conclusion is further supported by the different developmental timing of homeotic genes and intramuscular bone ossification: homeotic genes are expressed during the first few hours post-fertilization while intramuscular bone ossification does not occur until at least 4 days post-fertilization (Akimenko *et al*., 1994; Bird & Mabee, 2003; Yan *et al*., 2005).

Biomechanical function of myosepta and myoseptal tendons

The ossification of tendons in any animal is likely to have functional effects because changing the tissue character of a structure from collagenous tendons to the more compound material of bone also signifies a change in the material properties of this structure (reviewed by Dean, Swanson & Summers, 2009). While a tendon can be thought of as a spring, resisting tension but weak in torsion, compression, or bending, an ossified rod with the same shape as a collagenous tendon will be able to better resist forces in all directions.

The biomechanics of ossified tendons have been reviewed for ornithopod dinosaurs (Organ, 2006) and

birds (Berge & Storer, 1995) and there have long been hypotheses as to the function of sesamoid bones in humans (Mottershead, 1988). An analysis correlating postural changes in dinosaurs to the presence and location of ossified tendons showed that some tendons functioned to redistribute the stress of the body weight on the vertebrae while others did not appear to have such a function (Organ, 2006).

The function of the lateral tendons and of the entire horizontal septum in thunniform-bodied fish has been hypothesized to be direct force transmission between the axial musculature and the tail (Westneat *et al*., 1993; Donley *et al*., 2004). However, from these studies it appears that this morphological convergence occurs only at extreme body morphologies; there is no evidence that the function of myoseptal tendons is as straightforward as that of the more familiar muscle–tendon units in tetrapod limbs.

A hypothesis generated from the mechanics of undulatory aquatic locomotion is the modulation of myomere shape during contraction. If we assume that myomeres have near constant volume, as they contract and shorten along the length of their muscle fibres they must expand in other directions. On this basis, Brainerd & Azizi (2005) demonstrated that material properties of myomere boundaries can change the gear ratio of the muscle segment by changing the longitudinal shortening of the muscle relative to the shortening of the obliquely oriented muscle fibre. Additionally, many researchers have explored the role of intramuscular pressure in changing the body's flexural stiffness (Wainwright, Vosburgh & Hebrank, 1978; Long *et al*., 1996; Westneat *et al*., 1998; Pabst, 2000). Flexural stiffness is a significant mechanical property of undulating bodies that can dramatically alter their kinematics even under similar neuromuscular control and hydrodynamic conditions, with separate stiffness optima for peak acceleration and peak velocity (Tytell *et al*., 2010).

Flexural body stiffness in actively swimming fish has been a challenging metric to quantify. Researchers are thus focusing as much as possible on quantifying the material properties of the anatomical components comprising the fish body such as skin (Long *et al*., 1996) or vertebral column (Long *et al*., 1997; Porter *et al*., 2006). There is evidence that ossified myoseptal tendons may contribute to passive body flexural stiffness from an interesting case of convergent ossification not included in the analysed sample from Patterson & Johnson (1995). This appears to be the case in the knifefishes of the order Gymnotiformes (e.g. *Apteronotus albifrons*) and of the distant family Notopteridae (e.g. *Notopterus chitala*). The two families illustrate independent origins of anal fin swimming, during which the body is kept straight while the anal fin undulates. *Notopterus chitala* (Fig. 1D) has every tendon ossified, including the myorhabdoid (De Santana & Vari, 2010). Additionally, the epineural and epipleural tendons have a brush-like appearance probably due to the ossification of individual collagen fibres (Fig. 1E).

However, the same support for passive flexural stiffness is not provided by another group: the three-spined sticklebacks. Populations of three-spined stickleback, *Gasterosteus aculeatus*, vary in the extent to which their body surface is covered by bony scutes. Assuming insignificant changes in body shape, the varying degrees of body coverage would suggest different passive flexural stiffness. A review of museum specimens ($N = 10$) from two populations from the north-eastern United States shows that there is no clear correlation between the proportion of the body covered by dermal scutes and the proportion of the body covered by ossified epicentral tendons. A similar result was reached by Gemballa & Bartsch (2002) in a study of basal actinopterygians.

FUTURE DIRECTIONS

The myoseptal tendon system of teleosts has the potential to become an interesting model for the study of mechanical effects on bone development, given the many evolutionary origins and losses of tendon ossification within a diverse group of vertebrates. Many fundamentals, however, of intermuscular bone development have not been clarified. For example, what is the developmental origin of the tendon osteoprogenitor cells? Is mechanical loading required for normal intramuscular bone development?

Additionally, there is little information on the diversity of myoseptal shapes and how these correspond to different body types. Key in this effort will be to examine further the functional morphology of white muscle fibre arrangement as these make up the bulk of myomere muscle volume. White muscle fibres are arranged in a roughly helical pattern around the vertebral column (Alexander, 1969; Gemballa & Vogel, 2002) but because the determination of muscle fibre orientations and determination of localized muscle forces is such an onerous task, there is no comparative information to help us understand the functional implications of this arrangement. An extension of the model of Brainerd & Azizi (2005) to the more complex morphology of fishes, even with parallel muscle fibres, will be invaluable in determining whether there are regions of myosepta that consistently are under increased stress.

ACKNOWLEDGEMENTS

We thank Karsten Hartel and Andrew Williston of the Ichthyology collection, Jonathan Woodward of the

Digital Imaging Facility at the Harvard Museum of Comparative Zoology, and Valerie Percuoco for assistance provided during this study. We would also like to thank three anonymous reviewers for their constructive comments as well as Dr Sven Gemballa for his inspirational work in this field.

REFERENCES

Ahn D, Ho RK. 2008. Tri-phasic expression of posterior Hox genes during development of pectoral fins in zebrafish: implications for the evolution of vertebrate paired appendages. *Developmental Biology* **322:** 220–233.

Akimenko MA, Ekker M, Wegner J, Lin W, Westerfield M. 1994. Combinatorial expression of 3 zebrafish genes related to distal-less – part of a homeobox gene code for the head. *Journal of Neuroscience* **14:** 3475–3486.

Alexander RM. 1969. The orientation of muscle fibres in the myomeres of fishes. *Journal of the Marine Biological Association of the United Kingdom* **49:** 263–290.

Azizi E, Gillis GB, Brainerd EL. 2002. Morphology and mechanics of myosepta in a swimming salamander (*Siren lacertina*). *Comparative Biochemistry and Physiology A-Molecular and Integrative Physiology* **133:** 967–978.

Baldwin CC, Johnson GD. 1996. Interrelationships of aulopiformes. In: Stiassny MLJ, Parenti LR, Johnson GD, eds. *Interrelationships of fishes*. San Diego: Academic Press, 355–404.

Berge JCV, Storer RW. 1995. Intratendinous ossification in birds: a review. *Journal of Morphology* **226:** 47–77.

Bird NC, Mabee PM. 2003. Developmental morphology of the axial skeleton of the zebrafish, *Danio rerio* (Ostariophysi: Cyprinidae). *Developmental Dynamics* **228:** 337–357.

Brainerd EL, Azizi E. 2005. Muscle fiber angle, segment bulging and architectural gear ratio in segmented musculature. *Journal of Experimental Biology* **208:** 3249–3261.

Brainerd EL, Baier DB, Gatesy SM, Hedrick TL, Metzger KA, Gilbert SL, Crisco JJ. 2010. X-ray reconstruction of moving morphology (XROMM): precision, accuracy and applications in comparative biomechanics research. *Journal of Experimental Zoology Part A-Ecological Genetics and Physiology* **313A:** 262–279.

Chanet B, Chapleau F, Desoutter M. 2004. Intermuscular bones and ligaments in flatfishes [Teleostei : Pleuronectiformes]: phylogenetic interpretations. *Cybium* **28:** 9–14.

Chapman WM. 1944. The osteology of the Pacific deep-bodied anchovy, *Anchoa compressa*. *Journal of Morphology* **74:** 311–329.

Danos N, Fisch N, Gemballa S. 2008. The musculotendinous system of an anguilliform swimmer: muscles, myosepta, dermis, and their interconnections in *Anguilla rostrata*. *Journal of Morphology* **269:** 29–44.

De Santana CD, Vari RP. 2010. Electric fishes of the genus *Sternarchorhynchus* (Teleostei, Ostariophysi, Gymnotiformes); phylogenetic and revisionary studies. *Zoological Journal of the Linnean Society* **159:** 223–371.

Dean MN, Swanson BO, Summers AP. 2009. Biomaterials: properties, variation and evolution. *Integrative and Comparative Biology* **49:** 15–20.

DeSylva D. 1963. *Systematics and life history of the great barracuda, Sphyraena barracuda (Walbaum)*. Miami, FL: University of Miami Press, Institute of Marine Science.

Donley JM, Sepulveda CA, Konstantinidis P, Gemballa S, Shadwick RE. 2004. Convergent evolution in mechanical design of lamnid sharks and tunas. *Nature* **429:** 61–65.

Fine ML, Lin H, Nguyen BB, Rountree RA, Cameron TM, Parmentier E. 2007. Functional morphology of the sonic apparatus in the fawn cusk-eel *Lepophidium profundorum* (Gill, 1863). *Journal of Morphology* **268:** 953–966.

Gemballa S. 2001. Myoseptal tendons in vertebrates: spatial arrangement, functional and evolutionary implications. *American Zoologist* **41:** 1452–1452.

Gemballa S, Bartsch P. 2002. Architecture of the integument in lower teleostomes: Functional morphology and evolutionary implications. *Journal of Morphology* **253:** 290–309.

Gemballa S, Britz R. 1998. Homology of intermuscular bones in Acanthomorph fishes. *American Museum Novitates*, 25.

Gemballa S, Ebmeyer L, Hagen K, Hannich T, Hoja K, Rolf M, Treiber K, Vogel F, Weitbrecht G. 2003. Evolutionary transformations of myoseptal tendons in gnathostomes. *Proceedings of the Royal Society of London B* **1521:** 1229–1235.

Gemballa S, Roder K. 2004. From Head to Tail: The Myoseptal System in Basal Actinopterygians. *Journal of Morphology* **259:** 155–171.

Gemballa S, Treiber K. 2003. Cruising specialists and accelerators – are different types of fish locomotion driven by differently structured myosepta? *Zoology* **106:** 203–222.

Gemballa S, Vogel F. 2002. Spatial arrangement of white muscle fibers and myoseptal tendons in fishes. *Comparative Biochemistry and Physiology – Part A: Molecular & Integrative Physiology* **133:** 1013–1037.

Grande L, Bemis WE. 1998. A comprehensive phylogenetic study of amiid fishes (amiidae) based on comparative skeletal anatomy. An empirical search for interconnected patterns of natural history. *Memoir (Society of Vertebrate Paleontology)* **4:** iv–690.

Grandel H, Schulte-Merker S. 1998. The development of the paired fins in the Zebrafish (*Danio rerio*). *Mechanisms of Development* **79:** 99–120.

Hilton EJ. 2003. Comparative osteology and phylogenetic systematics of fossil and living bony-tongue fishes (Actinopterygii, Teleostei, Osteoglossomorpha). *Zoological Journal of the Linnean Society* **137:** 1–100.

Johnson GD, Patterson C. 1993. Percomorph phylogeny – a survey of acanthomorphs and a new proposal. *Bulletin of Marine Science* **52:** 554–626.

Kawahara R, Miya M, Mabuchi K, Lavoué S, Inoue JG, Satoh TP, Kawaguchi A, Nishida M. 2008. Interrelationships of the 11 gasterosteiform families (sticklebacks, pipefishes, and their relatives): a new perspective based on

whole mitogenome sequences from 75 higher teleosts. *Molecular Phylogenetics and Evolution* **46:** 224–236.

Lauder GV, Liem KF. 1983. The evolution and interrelationships of the actinopterygian fishes. *Bulletin of the Museum of Comparative Zoology* **150:** 95–197.

Lavoue S, Miya M, Nishida M. 2010. Mitochondrial phylogenomics of anchovies (family Engraulidae) and recurrent origins of pronounced miniaturization in the order Clupeiformes. *Molecular Phylogenetics and Evolution* **56:** 480–485.

Long J, Hale M, Mchenry M, Westneat M. 1996. Functions of fish skin: flexural stiffness and steady swimming of longnose gar, *Lepisosteus osseus*. *Journal of Experimental Biology* **199:** 2139–2151.

Long J, John H, Adcock B, Root RG. 2002. Force transmission via axial tendons in undulating fish: a dynamic analysis. *Comparative Biochemistry and Physiology – Part A: Molecular & Integrative Physiology* **133:** 911–929.

Long JH, Nipper KS. 1996. The importance of body stiffness in undulatory propulsion. *American Zoologist* **36:** 678–694.

Long JH, Pabst DA, Shepherd WR, McLellan WA. 1997. Locomotor design of dolphin vertebral columns: bending mechanics and morphology of *Delphinus delphis*. *Journal of Experimental Biology* **200:** 65–81.

Mabee PM, Crotwell PL, Bird NC, Burke AC. 2002. Evolution of median fin modules in the axial skeleton of fishes. *Journal of Experimental Zoology Part B-Molecular and Developmental Evolution* **294:** 77–90.

Moore JA. 1993. Phylogeny of the Trachichthyiformes (Teleostei, Percomorpha). *Bulletin of Marine Science* **52:** 114–136.

Mottershead S. 1988. Sesamoid bones and cartilages: an enquiry into their function. *Clinical Anatomy* **1:** 59–62.

Nelson JS. 2006. *Fishes of the world*. Hoboken, NJ: Wiley.

Nowroozi BN, Brainerd EL. 2010. Lateral bending kinematics of the vertebral column in *Morone saxatilis*. *Integrative and Comparative Biology* **50:** E126–E126.

Organ CL. 2006. Biomechanics of ossified tendons in ornithopod dinosaurs. *Paleobiology* **32:** 652–665.

Pabst DA. 2000. To bend a dolphin: convergence of force transmission designs in cetaceans and scombrid fishes. *American Zoologist* **40:** 146–155.

Pagel M. 1999. Inferring the historical patterns of biological evolution. *Nature* **401:** 877–884.

Patterson C, Johnson GD. 1995. The intermuscular bones and ligaments of teleostean fishes. *Smithsonian Contributions to Zoology* **559:** 1–84.

Porter HT, Motta PJ. 2004. A comparison of strike and prey capture kinematics of three species of piscivorous fishes: Florida gar (*Lepisosteus platyrhincus*), redfin needlefish (*Strongylura notata*), and great barracuda (*Sphyraena barracuda*). *Marine Biology* **145:** 989–1000.

Porter ME, Beltran JL, Koob TJ, Summers AP. 2006. Material properties and biochemical composition of mineralized vertebral cartilage in seven elasmobranch species (Chondrichthyes). *Journal of Experimental Biology* **209:** 2920–2928.

Ruvinsky I, Oates AC, Silver LM, Ho RK. 2000. The evolution of paired appendages in vertebrates: T-box genes in the zebrafish. *Development Genes and Evolution* **210:** 82–91.

Santini F, Harmon LJ, Carnevale G, Alfaro ME. 2009. Did genome duplication drive the origin of teleosts? A comparative study of diversification in ray-finned fishes. *BMC Evolutionary Biology* **9:** 194.

Santini F, Tyler JC. 2003. A phylogeny of the families of fossil and extant tetraodontiform fishes (Acanthomorpha, Tetraodontiformes), Upper Cretaceous to recent. *Zoological Journal of the Linnean Society* **139:** 565–617.

Schaeffer B, Patterson C. 1984. Jurassic fishes from the western United States, with comments on Jurassic fish distribution. *American Museum Novitates* **2796:** 1–86.

Shadwick RE, Gemballa S. 2006. Structure, kinematics, and muscle dynamics in undulatory swimming. In: Shadwick RE, Lauder GV, eds. *Fish biomechanics*, Vol. 23, London: Elsevier, 241–280.

Standen EM, Lauder GV. 2007. Hydrodynamic function of dorsal and anal fins in brook trout (*Salvelinus fontinalis*). *Journal of Experimental Biology* **210:** 325–339.

Tytell ED, Hsu CY, Williams TL, Cohen AH, Fauci LJ. 2010. Interactions between internal forces, body stiffness, and fluid environment in a neuromechanical model of lamprey swimming. *Proceedings of the National Academy of Sciences of the United States of America* **107:** 19832–19837.

Vallod D, Arthaud F. 2009. Intermuscular bones in common carps from six geographical French regions. *Cybium* **33:** 305–308.

Wainwright SA, Vosburgh F, Hebrank JH. 1978. Shark skin – function in locomotion. *Science* **202:** 747–749.

Ward AB, Brainerd EL. 2007. Evolution of axial patterning in elongate fishes. *Biological Journal of the Linnean Society* **90:** 97–116.

Webb PW. 1978. Fast-start performance and body form in 7 species of teleost fish. *Journal of Experimental Biology* **74:** 211–226.

Westneat MW, Hale ME, McHenry MJ, Long JH. 1998. Mechanics of the fast-start: muscle function and the role of intramuscular pressure in the escape behavior of *Amia calva* and *Polypterus palmas*. *Journal of Experimental Biology* **201:** 3041–3055.

Westneat MW, Hoese W, Pell CA, Wainwright SA. 1993. The horizontal septum – mechanisms of force transfer in locomotion of scombrid fishes (Scombridae, Perciformes). *Journal of Morphology* **217:** 183–204.

Yagashita N, Miya M, Yamanoue Y, Shirai SM, Nakayama K, Suzuki N, Satoh TP, Mabuchi K, Nishida M, Nakabo T. 2009. Mitogenomic evaluation of the unique facial nerve pattern as a phylogenetic marker within the perciform fishes (Telostei: Percomorpha). *Molecular Phylogenetics and Evolution* **53:** 258–266.

Yan YL, Willoughby J, Liu D, Crump JG, Wilson C, Miller CT, Singer A, Kimmel C, Westerfield M, Postlethwait JH. 2005. A pair of Sox: distinct and overlapping functions of zebrafish sox9 co-orthologs in craniofacial and pectoral fin development. *Development* **132:** 1069–1083.